Conformational Changes of *Robinia pseudoacacia* Lectin Related to Modifications of the Environment: FTIR Investigation

Josiane Wantyghem,*,‡ Marie-Hélène Baron,§ Michel Picquart,∥ and Françoise Lavialle⊥

Unité INSERM 180, UFR Biomédicale des Saints-Pères, 45 Rue des Saints-Pères, 75006 Paris, France, LASIR—CNRS, 8 Rue Henry-Dunant, 94320 Thiais, France, Laboratoire de Physique Moléculaire et Biologique, UFR Biomédicale des Saints-Pères, 45 Rue des Saints-Pères, 75006 Paris, France, and UPR 64—CNRS, UFR Biomédicale des Saints-Pères, 45 Rue des Saints-Pères, 75006 Paris, France

Received May 10, 1989; Revised Manuscript Received April 6, 1990

ABSTRACT: The secondary structural characteristics of one of the *Robinia pseudoacacia* lectins (RPA3) have been investigated by FTIR spectroscopy and have been established from absorption measurements in the amide I,I′ frequency range and from the quantitative estimation of the rate of NH ↔ N^2H exchange. In an anhydrous state the protein structure consists mainly of antiparallel and parallel β-structures, which represent 60% of the overall secondary structure of RPA3. Data obtained in different polar media (KBr, 2-chloroethanol, ^2H_2O, NaCl–^2H_2O and/or DPPC) reveal that RPA3 is a highly flexible protein. In pure ^2H_2O a rapid solvation of free peptide units and weak peripheral hydrogen bonds occurs, followed by the solvation of more internal parts of the lectin. The protein precipitates before total unfolding is reached. Increasing the ionic strength modifies the rate of NH ↔ N^2H exchange. NaCl concentrations of ≤0.15 M stabilize RPA3 in a structure close to that of the lyophilized lectin and diminish the rate of exchange, whereas higher NaCl concentrations partially disrupt the original secondary structure and increase the rate of exchange. Furthermore RPA3 was shown to interact with DPPC through polar interactions between the polar heads of the phospholipid and specific peptide units. These interactions appear to favor the NH ↔ N^2H exchange.

Lectins have been defined by and considered mostly for their binding to carbohydrate moieties. They are particularly useful to separate glycoproteins and glycopeptides and to probe changes in cell surface sugars during cell growth, differentiation, and malignancy. They have also been used to study the mitogenic stimulation of lymphocytes, which occurs at least partly through their binding to specific carbohydrate determinants present at the cell surface (Hume & Weidemann, 1980; Lis & Sharon, 1984). Nevertheless the physiological role of lectins remains largely speculative. Einhoff et al. (1986) have recently hypothesized that lectins would be engaged in the packaging of seed storage proteins. A survey of leguminous lectin sequences shows a high degree of conservation throughout evolution, possibly to ensure essential functions (Strosberg et al., 1986). Sequence homologies imply a close resemblance in the folding and three-dimensional structures of these proteins. β-pleated-sheet secondary structures appear as a characteristic of most lectins so far studied by X-ray crystallography, circular dichroism in the far-UV, or FTIR spectroscopy (Herrmann et al., 1978; Goldstein & Poretz, 1986) and would thus be important in the expression of lectin function. A systematic investigation of the structural properties of individual lectins should contribute to the understanding of their activities in situ.

Robinia pseudoacacia (RPA) seeds have been shown to contain a lectin that is highly mitogenic for human T lymphocytes (Sharif et al., 1977). The presence of several lectins in RPA seeds was reported only recently (Fleischmann & Rüdiger, 1986; Wantyghem et al., 1986). We have shown that these lectins present an immunological cross-reactivity but differ in their biochemical characteristics and in their biological activities. We have particularly described two of them, RPA1 and RPA3. Both are glycoproteins where the different carbohydrates (GlcNAc, Man, Xyl, Fuc) are present in approximately the same proportions but RPA1 is more highly glycosylated than RPA3 (12% vs 4.5%). From sedimentation equilibrium analysis and SDS–polyacrylamide gel electrophoresis, it can be concluded that RPA1 is a dimeric molecule of M_r 63 000 constituted of identical subunits whereas RPA3 is a tetramer of M_r 110 000 that contains two types of subunits of M_r 30 500 and 29 000. They exhibit quite different mitogenic dose–response curves, and RPA3 gives an optimal mitogenic stimulation at very low concentrations of lectin.

Except for a CD investigation performed by Père et al. (1975) before the existence of different RPA lectins was demonstrated, little information exists on RPA conformation. We have thus undertaken a structural investigation of RPA3, the most abundant lectin, by FTIR spectroscopy. From an accurate analysis of the amide I and amide II modes and from the kinetics study of the NH ↔ N^2H exchange of RPA3 peptide units, we define the secondary structure adopted by the lectin dissolved in various solvents. The structural modifications induced by increasing the ionic strength of the solvent and by introducing phospholipids are discussed.

Materials and Methods

Lectins. Robinia pseudoacacia lectins were isolated from black locust seeds as previously described (Wantyghem et al., 1986). The purified lectins were kept in sterile 0.15 M NaCl solutions at 4 °C, under which conditions they remained biologically active for more than 12 mo. Before FTIR experiments, RPA3 was exhaustively dialyzed against distilled water and lyophilized.

* To whom correspondence should be sent.
‡ Unité INSERM 180.
§ LASIR—CNRS.
∥ Laboratoire de Physique Moléculaire et Biologique.
⊥ UPR64—CNRS.

0006-2960/90/0429-6600$02.50/0

HPLC analyses showed that the tetrameric structure of RPA3 is maintained at the different salt concentrations.

Sample Preparation. The lyophilized RPA3 lectin was taken up in Fluorolube mulls (Sigma), KBr pellets, 2-chloroethanol (Merck), ^2H_2O (Sigma, 99.8% pure), 0.35 M SDS–^2H_2O, 0.05–0.5 M NaCl–^2H_2O, DPPC–^2H_2O, or DPPC–0.15 M NaCl–^2H_2O solutions. The lectin concentration in solutions was 4% (w/v), which corresponds to approximately 0.3 peptide unit/L. The p^{2}H (≅6.0) of the different solutions remained constant. SDS treatment was performed as follows: the protein sample was boiled for 2 min in 0.35 M sodium dodecyl sulfate (BDH) in ^2H_2O and kept for at least 24 h at room temperature before spectra were recorded.

The RPA3–DPPC sample was prepared under the following conditions. The aqueous RPA3 lectin was added to DPPC (Sigma) multilayers at a molar ratio of 1:300 in H_2O (≅3 peptide units/L DPPC). The lipid–protein mixture was lyophilized and then taken up either in ^2H_2O or in 0.15 M NaCl–^2H_2O.

Infrared Measurements. FTIR spectra were recorded at room temperature with a Nicolet 5 DX FTIR spectrophotometer equipped with a globar source and a TGS (triglycine sulfate) detector. An air-dryer was used to purge the instrument. Samples were held in a transmission cell of 25-μm path length fitted with CaF_2 window.

For each spectrum, 100 interferograms were collected in 100 s at 4-cm^{-1} resolution. The infrared spectra were recorded within 10 min after the addition of the solvent and at different times up to 24 h.

IR spectra were corrected by subtracting the solvent absorption in order to obtain a straight base line from 1850 to 1350 cm^{-1}. This subtraction further minimizes the water vapor absorption.

Mathematical Procedure. (1) Curve-Fitting Analysis. The various amide I,I′ (or amide I* to design both) and amide II,II′ modes corresponding to the major conformations that a protein may adopt, i.e., α-helix, parallel and antiparallel β-pleated sheets, turns, nonrepetitive arrangements, and those resulting from the direct interactions between peptide units and solvents are largely overlapping. Moreover amino acid side-chain absorptions may also contribute to these bands. To process such complicated data the bands obtained in the 1850–1350-cm^{-1} interval were decomposed directly in nine Lorentzians by means of a least-squares fitting program; three adjusting parameters (frequency, intensity, bandwidth at half-height) were considered for each Lorentzian. An initial bandwidth at half-height of 40 cm^{-1} was attributed to each Lorentzian. The frequency and intensity of each absorbance maximum of the original spectrum were considered as the frequency and intensity of the main component of the band. The initial intensities and frequencies of the other components were chosen in order to give the best adjustment, and each assay was visualized before calculation was initialized. The fitting adjustment was performed until the synthetic curve matched the experimental one with a precision factor of ≤1%. Such a precision factor was reached when the number of Lorentzians was at least equal to nine. Decreasing the number of Lorentzians leads to a lower precision factor whereas increasing this number makes difficult the attribution of the different bands. Consequently the number of Lorentzians was limited to nine. In the fitting procedure signals over 1700 cm^{-1}, which can be attributed to carboxylic νCO of the protein and/or to the ester CO of DPPC, have not been considered. Decomposed spectra thus give a straight line between 1850 and 1700 cm^{-1}. The four bands obtained in the 1700–1600-cm^{-1} range were attributed to amide I,I′ absorptions. The remaining components were assigned to the amide II and ν_a COO^- absorptions when they occurred between 1600 and 1500 cm^{-1}, and to amide II′, ν_s COO^- and CH deformation absorptions between 1500 and 1400 cm^{-1}.

The percentages corresponding to the relative surface of each Lorentzian were determined in the three frequency ranges reported above in order to compare the different decomposed spectra. The various structures displayed in the amide I* region are supposed to have close molar extinction coefficients (Chirgadze et al., 1973), therefore their fractional areas are generally considered as representative of the relative proportions of the conformational structures adopted by a given protein (Byler & Susi, 1986; Surewicz & Mantsch, 1988).

To increase the signal to noise ratio, Fourier self-deconvolution or derivation was performed on smoothed spectra according to Kauppinen et al. (1981). The spectra were band-narrowed by Fourier self-deconvolution using a 40 cm^{-1} bandwidth Lorentzian line at half-height and a resolution enhancement factor of 2.5. Such a large bandwidth allows one to take into account the enlargement of the different components due to the presence of both amide I and amide I′ components, which coexist when the hydrogen–deuterium exchange is not completed. Under such conditions the weak bands of water vapor ($\nu_{1/2max} \cong 2$ cm^{-1}), which may persist on difference spectra, will not affect significantly the self-deconvoluted and second-derivative spectra and, in any case, will not modify the number of the main bands.

(2) Determination of the NH ↔ N^{2}H Exchange. Amide I* and amide II heights were measured from a base line drawn between 1850 and 1350 cm^{-1}. The NH ↔ N^{2}H exchange was determined from the height of the amide II peak in each solvent (I_S) according to the following formula:

$$[1 - (I_S - I_{SDS})/(I_F - I_{SDS})] \times 100 \quad (1)$$

The different amide II heights used in eq 1 were normalized with respect to a constant height for the amide I* band which was supposed to be relatively insensitive to the deuteration process. I_F represents the maximum intensity of the amide II band in Fluorolube (nonexchanged protein, 0% N^{2}H). I_{SDS} represents the minimum intensity of the amide II band in SDS–^2H_2O (fully exchanged protein, 100% N^{2}H).

Results and Discussion

Structural Characterization of RPA3

(1) General Remarks. The effects of protein solvation prove to be rather complex. A close examination of the different frequencies of the amide I,I′ and II,II′ modes reported in the literature and their correlation to a given structure or interactions appears of interest. Table Ia summarizes the different amide I* and amide II frequency ranges that have been associated with the well-known protein–secondary structures. The frequencies of the amide I* and amide II modes relevant to direct interactions between peptide units and solvents are reported in Table Ib. The frequencies observed in the same range for the amino acid side chains are given in Table Ic (for references see Table I).

From Table I, it has been assumed that absorptions between 1660 and 1700 cm^{-1} are essentially related to non-hydrogen-bonded amide CO groups involved in random coils, turns, and β-strands (de Lozé et al., 1978). These CO groups will be referred as "free" CO groups. Absorptions between 1640 and 1670 cm^{-1} partially overlap the former frequency range. They are associated with hydrogen-bonded peptide units in α-helix, turns, and random coils (Byler & Susi, 1986; Krimm & Bandekar, 1986) but are also relevant to CO···^2H_2O or

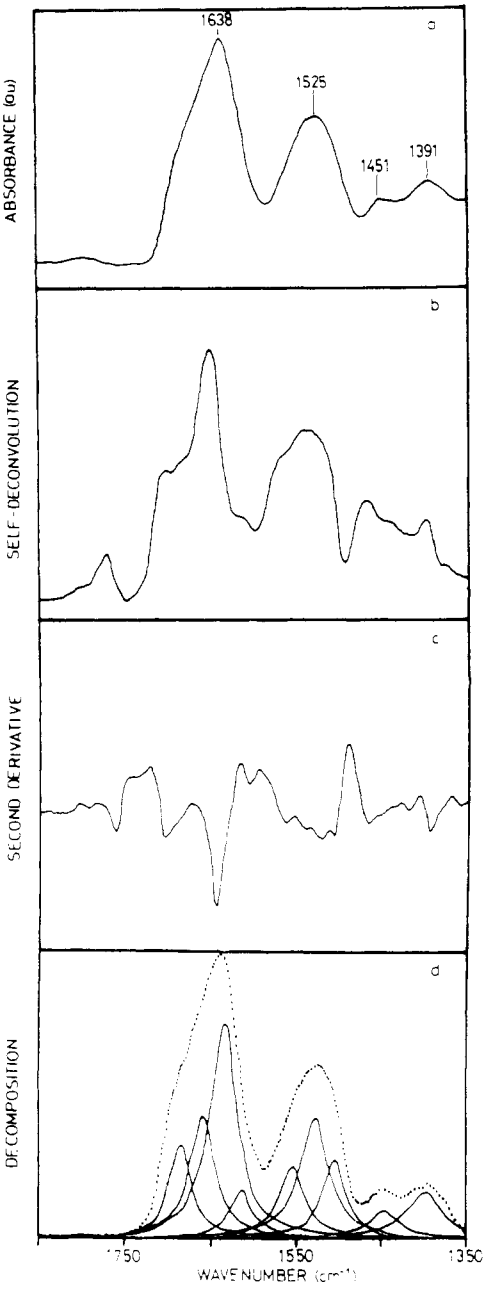

FIGURE 1: IR spectrum of RPA3 in Fluorolube mulls. Lyophilized RPA3 (2 mg) was suspended in Fluorolube and the spectrum was recorded in the 1850–1350-cm^{-1} frequency range. (a) Original unsmoothed spectrum. (b) Deconvolved spectrum. (c) Second-derivative spectrum. (d) Decomposed spectrum.

$CO\cdots Na^+$ (or K^+) interactions (Baron et al., 1973; de Lozé et al., 1978). Amide I* frequencies in the 1626–1640-cm^{-1} range are attributed to parallel β-sheets (Bandekar & Krimm, 1988a,b) but could as well be assigned to antiparallel β-strands (1612–1640 cm^{-1}) (Susi & Byler, 1987). Peptide units involved in $Na^+\cdots(C)O\cdots{}^2H_2O$ interactions are also expected to absorb in this frequency range (Baron et al., 1973; de Lozé et al., 1978; Biay et al., 1989). Finally, the amide I* frequencies of antiparallel β-sheets of large size, which involve multistrands (Krimm & Bandekar, 1986) as well as those associated with $CO\cdots({}^2H_2O)_2$ interactions (Baron et al., 1973; de Lozé et al., 1978), are expected between 1610 and 1635 cm^{-1}. Absorption bands of the amino acid side chains (Asn, Gln, Arg, Tyr) are weak compared to the amide I* mode (Chirgadze et al., 1975) and may be disregarded in the 1700–1600-cm^{-1} frequency range (Eckert et al., 1977), whereas the contribution of ionized Asp and Glu side chains may be

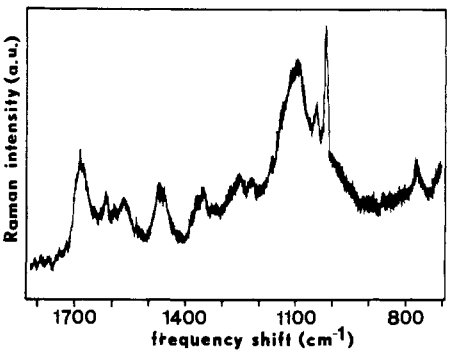

FIGURE 2: Raman spectrum of RPA3. The spectrum of the lyophilized lectin was recorded at room temperature. Excitation wavelength, 514.5 nm; power, 400 mW; resolution, 4 cm^{-1}.

significant in the amide II region especially when the intensity of this mode strongly decreases in ^2H_2O solutions.

(2) RPA3 Conformation in Anhydrous Media. (2-1) RPA3 in Fluorolube. Figure 1a displays the IR spectrum in the 1850–1350-cm^{-1} range of RPA3 suspended in Fluorolube, an apolar medium. Two main peaks culminating at 1638 and 1525 cm^{-1} were observed. The bandwidth at half-height of the amide I feature is rather large (79 cm^{-1}), which suggests that various conformations are overlapping.

The two less intense spectral features centered at 1446 and 1401 cm^{-1} were respectively assigned to the C–H bending vibrations of the amino acid side chains and to the ν_s COO^- modes of Glu and Asp residues (Perchard et al., 1984; Krimm & Bandekar, 1986).

After mathematical treatments of the amide I band (Figure 1b–d, Table II), the major feature was centered at ca. 1635 cm^{-1}. This frequency is too low to be associated with α-helix conformations or random coil structures but too high to be assigned to antiparallel β-pleated multistrand structures of large size. It might be rather associated with parallel β-pleated sheet conformations and/or antiparallel β-strands of small size, for instance, double strands. According to the decomposed spectrum (Figure 1d), the component around 1620 cm^{-1} could account for a weak amount of antiparallel β-sheets of large size. This component may be related to the shoulder around 1600 cm^{-1} observed after self-deconvolution or second derivation (Figure 1b,c). This may reflect that the amide I absorptions of antiparallel β-structures of large size are dispersed. In the three processed spectra, the component around 1685 cm^{-1} should correspond to hydrogen-bonded CO groups involved in β-sheet structures but also to "free" CO groups located in turns, unordered structures, and β-structures of small size. The band or shoulder at ca. 1660 cm^{-1} could be assigned to hydrogen-bonded CO groups involved in nonregular conformations, i.e., turns and random coils. An α-helix content would contribute to the intensity of the lower frequency side of these weak features. Raman spectroscopy provides additional evidence that RPA3 adopts mainly β-pleated-sheet conformations, since the maximum of the amide I peak is centered at 1675 cm^{-1} (Figure 2).

IR amide II frequencies (Table II) further support the above conclusions, since parallel β-sheets, antiparallel β-double strands, and turns could give rise to the 1556- and 1533-cm^{-1} peaks whereas the absorption at 1512 cm^{-1} would result from larger antiparallel β-sheets and from "free" NH groups located in protein domains close to the "free" peptide CO groups.

(2-2) RPA3 in KBr. The spectrum of RPA3 in KBr pellets (Figure 3a) exhibits an extremely broad amide I band centered at 1660 cm^{-1} with a bandwidth at half-height of $\cong$110 cm^{-1}, which suggests an enhancement of random structures. Com-

Table I: Frequency at Maximum Absorbance (ν) of the Different Amide Band Components in the 1700–1400-cm^{-1} Frequency Range[a]

	ν (cm^{-1})		
	amide I[b]	amide II	amide II′
	(a) Protein–Secondary Conformation		
α-helix	1657–1645	1550–1537 (strong)	1488
		1520–1510 (shoulder)	1464
antiparallel β-pleated sheet	1699–1670 (weak)	1555 (weak)–1560	1485–1464
	1640–1612 (strong)	1530–1510 (strong)	
parallel β-pleated sheet	1642–1626	1553–1530	1480
random coil	1654–1640	1540–1530	
turns[c]	1696–1681	1565–1530	
	1675–1655		
	(b) Peptide Unit–Solvent Interactions		
apolar solvent	1680–1665	1500 (medium)	1418
		1515 (shoulder)	1438
$C{=}O\cdots {}^2H_2O$	$\simeq$1650		
$C{=}O$ with ^2H_2O	$\simeq$1620		
$C{=}O\cdots Na^+$	$\simeq$1654		
$C{=}O$ with Na^+ and ^2H_2O	$\simeq$1635		

		assignment	ν (cm^{-1})	ϵ (L·mol^{-1}·cm^{-1})[e]
		(c) Amino Acid Side-Chain Absorption[d]		
Asp, Glu	COO^2H	ν CO	1714, 1706	$\simeq$300
	COO^-	ν_a COO^-	1584, 1567	$\simeq$800
		ν_s COO^-	1405	
Asn, Gln	$CO(N^2H_2)$	ν CO	1648, 1635	$\simeq$550
Arg	$(^2H_2N{-}C{=}N^2H_2^+)$	ν_a, ν_s N—C=N	1608, 1586	$\simeq$500
Tyr		ν squelette	1515	$\simeq$500

[a] This table summarizes the compilation of the following references. Part a: Bandekar and Krimm (1988a,b), Byler and Susi (1986, 1988), Chirgadze et al. (1973), Chirgadze and Nevskaya (1976), Jackson et al. (1989), Krimm and Bandekar (1986), Surewicz and Mantsch (1988), Susi and Byler (1987). Part b: Baron et al. (1973, 1978), Biay et al. (1989), Fillaux and de Lozê (1972), de Lozê et al. (1978). Part c: Chirgadze et al. (1975), Perchard et al. (1984). [b] A shift of $\simeq$5 cm^{-1} toward lower frequencies is expected between the amide I (–CONH–) and the amide I′ (–CON^{2}H–) modes. The amide I frequency ranges have been chosen to include both possibilities. [c] Turns (β, γ) involve "free" C=O groups and hydrogen-bonded C=O groups (Krimm & Bandekar, 1986). [d] Only absorptions with an $\epsilon \geq 200$ L·mol^{-1}·cm^{-1} have been reported. [e] Molar absorption coefficient at ν_{max}.

Table II: Frequencies and Fractional Areas in the 1850–1350-cm^{-1} Range of the IR Spectrum of RPA3 in Different Media

	ν (cm^{-1})[a]			
frequency range (cm^{-1})	Fluorolube	KBr	2-chloroethanol	SDS–^2H_2O
1710–1600		1706 (7)		
	1684 (15)	1682 (18)		
			1671 (25)	1677 (8)
	1662 (25)			1660 (22)
		1655 (45)	1657 (13)	
			1647 (48)	
	1638 (51)			1641 (39)
	1618 (9)	1616 (30)	1625 (14)	1620 (31)
1600–1500				1586 (61)
	1556 (26)	1553 (55)	1556 (8)	1556 (39)
			1546 (51)	
	1533 (49)	1528 (20)		
			1521 (41)	
	1512 (25)			
		1505 (25)		
1500–1400				1491 (7)
			1466	1461 (59)
		1454 (77)		
	1446 (38)			1440 (34)
			1419	
	1401 (62)	1404 (23)		
amide I,I* bandwidth at half-height (cm^{-1})	79	110	53	68

[a] Numbers in parentheses are fractional areas.

pared to Fluorolube, the KBr polar medium could promote a particular secondary structure as well as disrupt hydrogen bonds. The results reported in Table II are in agreement with self-deconvolution and second derivation (data not shown). They reflect two effects: (i) the increase in the feature around 1620 cm^{-1} indicates that the antiparallel β-sheet structures of large size are probably favored in KBr; (ii) the shift of the major band from ca. 1638 cm^{-1} in Fluorolube to ca. 1655 cm^{-1}

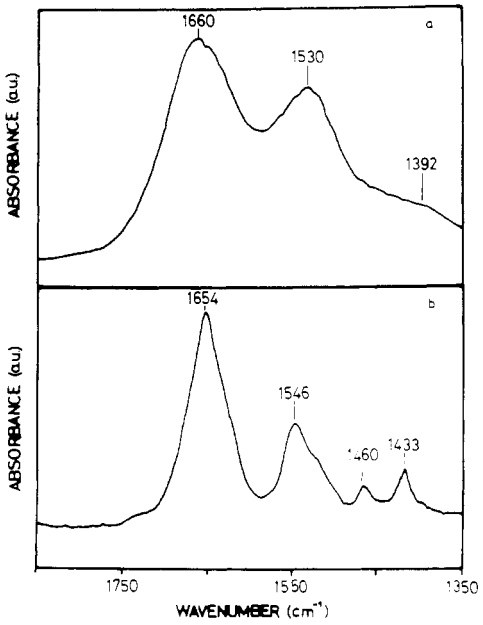

FIGURE 3: IR spectra of RPA3 in KBr pellets and in 2-chloroethanol. (a) Lyophilized RPA3 (2 mg) in KBr pellets. (b) RPA3 solvated in 2-chloroethanol (lectin concentration, 40 mg/mL).

in KBr pellets shows that ionic interactions between K^+ and CO groups and between Br^- and NH groups may replace a part of the hydrogen bonds previously involved in β-structures absorbing at 1638 cm^{-1}, thus increasing the random conformations. An α-helix enhancement would have narrowed rather than broadened the amide I band.

Likewise, analysis of the amide II region gives results that are quite different from those obtained with Fluorolube mulls and confirms the large changes of the secondary structures between the two media. However, the decomposed amide II range related to KBr pellets appears difficult to discuss without any accurate data on amide II frequencies related to peptide NH–Br^- interactions.

The band or shoulder that appears at ca. 1706 cm^{-1} for the three mathematical treatments was attributed to the carboxylic forms of Asp and Glu side chains. This was correlated to the relative decrease of the carboxylate forms absorbing at ca. 1401 cm^{-1} in Fluorolube. This indicates that KBr medium also affects the tertiary structure of RPA3.

From these observations it seems clear that Fluorolube constitutes a better reference than KBr pellet to examine RPA3 conformations when the protein does not interact with its environment.

(2-3) RPA3 in 2-Chloroethanol. 2-Chloroethanol is known as an α-helix-promoting agent (Herskovits & Mescanti, 1965) and was thus used as a standard to determine whether RPA3 might adopt such a conformation. Under these experimental conditions (Figure 3b), the amide I absorption shifts toward higher frequencies (1654 cm^{-1}). Furthermore, this frequency shift is associated with a pronounced narrowing in the amide I bandwidth at half-height from 79 to 53 cm^{-1}. These data suggest a large increase of the α-helix content of RPA3 in 2-chloroethanol compared to that observed in Fluorolube.

After mathematical processing of the original spectrum, the major symmetrical peak centered around 1650 cm^{-1} in all cases confirms the existence of a predominant α-helical conformation. The strong amide II component of ca. 1548 cm^{-1} further supports the formation of α-helical structures.

The weak absorptions of ca. 1625 and 1520 cm^{-1} (Table II), which are related to shoulder or peak on self-deconvolution or second derivation (not shown), emphasize the presence of

Table III: Frequencies and Fractional Areas in the Amide I* Band of the IR Spectrum of RPA3 Solvated in Different Media[a]

medium	amide I,I′ frequency (cm^{-1})				amide I,I′ bandwidth at half-height (cm^{-1})
^2H_2O	1675 (5)	1657 (23)	1635 (58)	1611 (15)	59
0.05 M NaCl–^2H_2O	1678 (7)	1655 (25)	1636 (56)	1611 (12)	64
0.5 M NaCl–^2H_2O	1676 (6)	1658 (22)	1636 (60)	1616 (12)	59
DPPC–^2H_2O	1675 (13)	1657 (15)	1639 (60)	1620 (12)	59
DPPC–NaCl–^2H_2O	1672 (12)	1657 (12)	1641 (54)	1624 (22)	61
Fluorolube	1684 (15)	1662 (25)	1638 (51)	1618 (9)	79

[a] Spectra were recorded within 10 min after addition of the solvent. Fractions of the total amide I* (amide I,I′) absorbance for each solvent are given in parentheses and are referred to the values obtained in Fluorolube mulls.

rather large and stable antiparallel β-sheets. However, the relative intensity of the absorption at ca. 1670 cm^{-1} is clearly too important to account for these structures only. As in Fluorolube, these absorptions could be associated with "free" CO groups. The shift toward lower frequency in 2-chloroethanol could be due to the difference of solvent polarities (Baron et al., 1978). The weak amide I component at 1657 cm^{-1} and the amide II component at 1556 cm^{-1} probably arise from turns and random structures. In the amide II range, the absorption at 1521 cm^{-1} (Table II) may account for "free" peptide NH groups more or less solvated by 2-chloroethanol. The peak attributed to ν_s COO^-, which is now located at ca. 1420 cm^{-1}, clearly indicates that a significant perturbation of the carboxylate side chains occurred.

(3) RPA3 Conformation in Aqueous Solutions. When RPA3 is solvated in deuterated water, the NH $\leftrightarrow$ N^2H exchange should lead to a decrease of the amide I frequencies of $\cong$5 cm^{-1} independently of any structural change (Byler & Susi, 1986). Hence, a shift of the previous amide I peak toward lower frequencies ($\rightarrow$ amide I′) exceeding 5 cm^{-1} or a fortiori toward higher frequencies will reflect a solvent effect on RPA3 conformation. The amide II peak was considered irrelevant to analyze conformational changes since, in deuterated water, a progressive decrease of this peak is observed with a concomitant increase of the amide II′ peak at ca. 1460 cm^{-1}.

(3-1) RPA3 in ^2H_2O. The IR spectrum of RPA3 solvated for 10 min in ^2H_2O (Figure 4a) exhibits three peaks in the 1850–1350-cm^{-1} interval with maxima at 1642, 1544, and 1457 cm^{-1}. The bandwidth at half-height of the amide I* band is narrower than in Fluorolube (59 cm^{-1}). Compared to Fluorolube, the above spectrum shows that the amide I* frequency slightly increased.

After the different mathematical processings, the intensity of the highest frequency component decreased relatively (Figure 4b–d, Table III). This indicates that a part of the CO groups, which were "free" in Fluorolube, become deuterium or hydrogen bonded in ^2H_2O. Consequently, either the percentage of β-structures increases (see Table Ia) or direct CO···$(^2H_2O)_{1-2}$ interactions are formed (see Table Ib) or both. However, it could be assumed that the conformation of the lyophilized lectin is largely maintained in ^2H_2O during the first 10 min of solvation.

(3-2) RPA3 in NaCl–^2H_2O. In the amide I* range, spectra of RPA3 solvated in 0.05 or 0.5 M NaCl–^2H_2O (not shown)

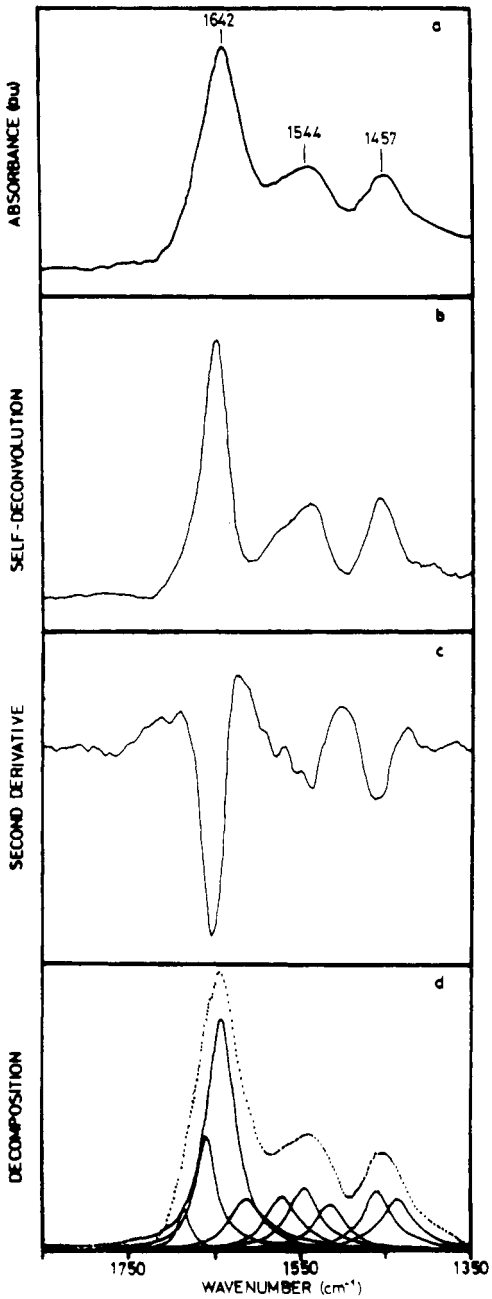

FIGURE 4: IR spectrum of RPA3 in ^2H_2O. Lectin concentration, 40 mg/mL. Spectrum was recorded after 10 min of solvation in ^2H_2O. (a) Original unsmoothed spectrum. (b) Deconvolved spectrum. (c) Second-derivative spectrum. (d) Decomposed spectrum.

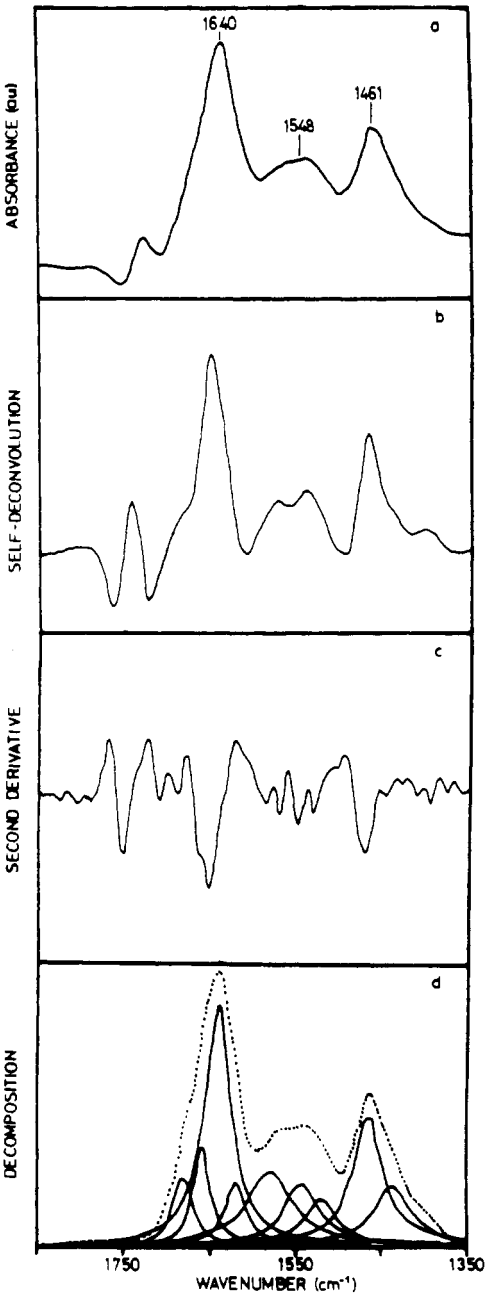

FIGURE 5: IR spectrum of RPA3 in DPPC–^2H_2O. Lectin concentration, 40 mg/mL; DPPC concentration, 50 mg/mL; RPA3/DPPC = 1/300. Spectrum was recorded after 10 min of solvation in ^2H_2O. (a) Original unsmoothed spectrum. (b) Deconvolved spectrum. (c) Second derivative spectrum. (d) Decomposed spectrum.

are close to that obtained in ^2H_2O. After decomposition, as already observed in pure ^2H_2O, the amide I* component of highest frequency decreases in intensity (Table III).

From these results we assume that, as in pure ^2H_2O, a part of the initially "free" CO peptide groups become involved in new interactions that give rise to the increased absorption at ca. 1636 cm^{-1}.

Whether these new interactions correspond at the peptide level to an increase of the small size β-structures (ca. 1636 cm^{-1}) (Table Ia) or whether they correspond to the formation of combined $Na^+\cdots(C)O\cdots^2H_2O$ interactions (Table Ib) remains unclear from these unique data.

(3-3) RPA3 Solvated in Deuterated Solutions in the Presence of DPPC. The particular feature observed between 1750 and 1700 cm^{-1} on the difference spectrum between RPA–3–DPPC–^2H_2O and DPPC–^2H_2O (Figure 5a) is characteristic of a shift to lower frequencies of the νCO modes of the DPPC multilayers (Surewicz et al., 1987; Blume et al., 1988). This unambiguously indicates that RPA3 perturbs at least the polar heads of the phospholipids.

After mathematical analyses (Figure 5b–d) and compared to pure ^2H_2O, the band at 1675 cm^{-1}, which was essentially assigned to "free" CO peptide groups, becomes complex and increases in intensity whereas band components or shoulders at ca. 1655 cm^{-1} (CO involved in turns and random structures) seem to decrease. This suggests that, in the presence of DPPC, hydrogen-bonded CO groups in turns or in unordered parts of RPA3 become partly "free". This could result from the disruption of peptide CO···NH bonds when NH groups come in interactions with either HPO_4^- or CO-ester groups of DPPC.

In the presence of NaCl, the intensities of the bands at ca. 1675 and 1657 cm^{-1} are not significantly modified (Table III). In contrast, NaCl induces changes in the relative intensities of the two lowest amide I* bands. It could be proposed that

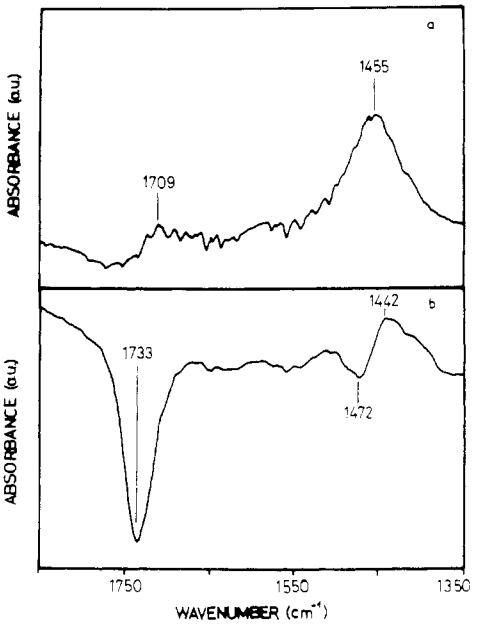

FIGURE 6: Difference spectrum of DPPC–NaCl–^2H_2O and DPPC–^2H_2O. DPPC concentration, 50 mg/mL in ^2H_2O or in 0.15 M NaCl–^2H_2O. (a) Canceling the absorption band due to the carbonyl group at $\cong$1730 cm^{-1}; (b) canceling the absorption band due to the aliphatic chain at $\cong$1460 cm^{-1}.

DPPC–NaCl–^2H_2O modifies the repartition between the various possible β-structures. However, this may be also associated to a change in the amount of ^2H_2O-bonded CO peptide group interactions due to the presence of CO···^2H_2O species.

Moreover, it should be pointed out that NaCl induces a perturbation on the lipid organization as shown by the difference spectrum between DPPC–NaCl–^2H_2O and DPPC–^2H_2O (Figure 6), which indicates that NaCl perturbs both the carbonyl groups and the aliphatic chains of DPPC as reported by Lotta et al. (1988).

Analysis of the NH ↔ N^2H Exchange

(1) Preliminary Remarks. As reported for many proteins, the hydrogen–deuterium exchange of the NH peptide groups of RPA3 was examined to give an insight into the molecular conformation of this protein and to provide information on the conformational dynamics of RPA3 in solution (Gregory & Rosenberg, 1986; Kim, 1986). The rate of NH ↔ N^2H exchange depends on the accessibility of the NH groups to ^2H_2O. This accessibility is limited by the presence of hydrogen bonds and/or by the location of the NH groups in the protein core. However, it can be assumed that, once a peptide NH group comes into direct contact with ^2H_2O, the NH ↔ N^2H chemical-exchange reaction occurs rapidly by one of the following processes: acid or basic catalysis, or direct ^2H_2O exchange (Gregory & Rosenberg, 1986). NH groups involved in turns or random coils are either "free" or hydrogen bonded. These latter bonds are supposed to be less stable than those which stabilize cooperatively the secondary stereoregular structures i.e., α-helix, parallel and antiparallel β-sheets. Furthermore, secondary structures that involve a large number of hydrogen bonds are supposed to be more stable than those only fixed by a few hydrogen bonds. It thus results that "free" NH groups located in outer parts of the protein should exchange first. Then, when the intake of ^2H_2O or ions becomes sufficient to locally disrupt hydrogen bonds, NH groups involved in turns or random parts of RPA3 or in regular structures of small size may exchange, depending on their location in the protein.

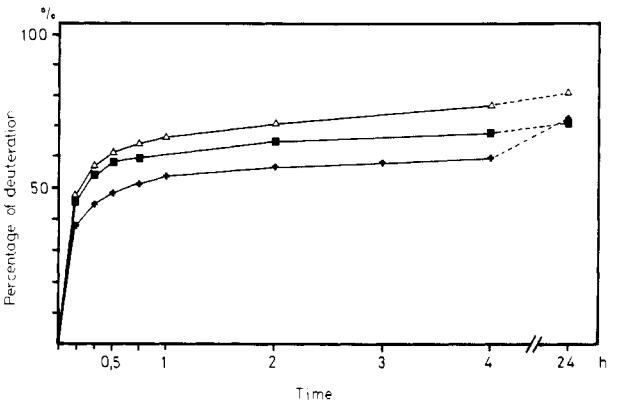

FIGURE 7: Percentages of deuteration of RPA3 vs time of solvation in the presence of DPPC. +, ^2H_2O; ■, DPPC–^2H_2O; △, DPPC–0.15 M NaCl–^2H_2O. The percentage of deuteration was determined according to eq 1 given in Materials and Methods.

Regular structures of large size will exchange only if the rest of the protein backbone becomes entirely solvated through a major cooperative unfolding. All these observations indicate that NH ↔ N^2H exchange rates are extremely sensitive both to the local chemical environment of the exchange sites and to the overall conformational dynamics of the proteins. Moreover, it has been proved that exchange rates also depend on the solvent characteristics (pH, ionic strength, viscosity) and on the temperature (Kim & Baldwin, 1982; Gregory & Rosenberg, 1986).

(2) Analysis of the NH ↔ N^2H Exchange as a Function of Time. In part A we have shown that RPA3 would contain "free" peptide CO groups ($\cong$1680 cm^{-1}), weakly hydrogen-bonded ones probably involved in turns and randomly coiled structures ($\cong$1660 cm^{-1}), a relatively large amount of parallel and/or antiparallel β-strands ($\cong$1636 cm^{-1}), a minor amount of larger antiparallel β-sheets ($\cong$1615 cm^{-1}), but no detectable α-helix.

In all the solvents used the deuteration process of RPA3 may be approximately divided in three parts: 0–10 min, 10 min–1 h, and 1–24 h.

(2-1) RPA3 in ^2H_2O. Figure 7 shows that $\cong$40% of the NH groups are deuterated at 10 min. In part A-3-1 we concluded that peptide CO groups that were "free" in Fluorolube became complexed in pure ^2H_2O (Table III). A corresponding amount of NH groups is assumed to exchange rapidly. The NH groups exchanged subsequently should correspond to external weakly hydrogen-bonded peptide units located in turns, random coils, or β-structures of small size. From 10 min to 1 h the proportion of N^2H increases of approximately 15%. This suggests that additional external β-structured parts of RPA3 are then disrupted. Consequently, no more than 15% of the β-structures of small size (Table III) should be located in external parts of RPA3. A part of the buried hydrogen-bonded NH groups located in polar internal regions of RPA3 are supposed to correspond to the next 20% of exchange observed between 1 and 24 h. These results could be explained if a significant fraction of previously hydrogen-bonded peptide units are alternatively involved in CO···^2H_2O or CO···$(^2H_2O)_2$ interactions. After 24 h, the remaining 28% unexchanged NH groups are associated with peptide units involved in apolar regions of RPA3. They should consist of residual β-structures of small size and of antiparallel β-sheets of larger size that would never be in direct contact with ^2H_2O.

(2-2) RPA3 in NaCl–^2H_2O Solutions. Figure 8 shows that the NH ↔ N^2H exchange largely depends on salt concentrations. Compared to the results obtained in pure ^2H_2O, when the salt concentration is low ($\leq$0.15 M) some peptide units

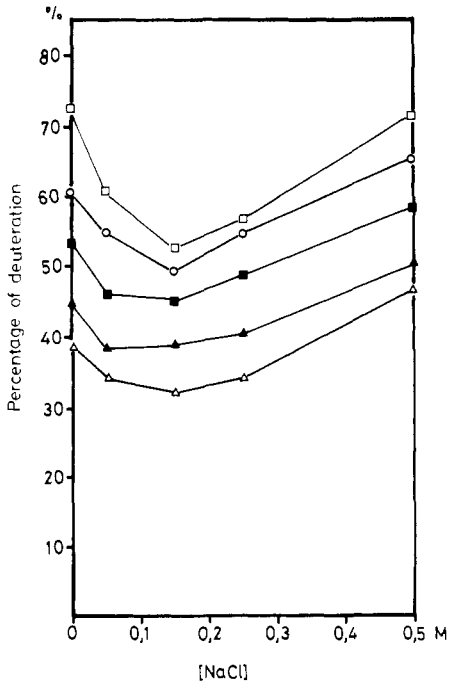

FIGURE 8: Percentages of deuteration of RPA3 vs NaCl concentrations as a function of time. △, 10 min; ▲, 20 min; ■, 60 min; ○, 4 h; □, 24 h.

estimated to 4% (0.05 M NaCl) and to 6% (0.15 M NaCl) are protected against the exchange during the first 10 min. The relative amount of protected NH groups slightly increases at 1 h (8%). From 1 to 24 h it reaches 12% for 0.05 M NaCl and 20% for 0.15 M NaCl. In contrast, for 0.5 M NaCl solutions the percentage of deuteration at 10 min is larger than in pure ^2H_2O (≅8%). This excess of N^{2}H decreases to 5% at 4 h and finally, at 24 h, this percentage becomes similar to that in pure ^2H_2O. Intermediate results are observed in 0.25 M NaCl. The NH ↔ N^{2}H exchange may be affected by NaCl concentrations in two different ways: either a direct effect on the rapid exchange of NH groups solvated by hydrated Cl^- anions instead of pure ^2H_2O or an indirect effect associated with slow structural modifications of RPA3. As we discuss mostly the kinetics exchange that occurs after 10 min we assume that the salt effect results essentially from modifications of RPA3 structure. The following explanation should be proposed: low amounts of NaCl (≤0.15 M) interacting with the polar side chains of the protein would stabilize the tertiary structure of RPA3. Under these conditions, NaCl would prevent ^2H_2O molecules from penetrating inside the protein and limit the partial aggregation of apolar amino acid side chains in avoiding the disruption of internal β-structures. In contrast, at higher salt concentrations, 0.5 M NaCl for instance, NaCl would interact rapidly not only with amino acid side chains but also might dissociate some of the weakly hydrogen-bonded peptide units at the protein surface. RPA3 is apparently more rapidly denaturated in 0.5 M NaCl than in pure ^2H_2O, but after 24 h the nonhydrated structured part of the molecule remains the same as in pure ^2H_2O (28%). At this time the conformational change of RPA3 is not larger in pure ^2H_2O than in 0.5 M NaCl–^2H_2O. All these data may be explained if the hypothesis of the formation of peptide units–salt–^2H_2O interactions in the presence of high NaCl concentrations is favored against that of an increase of β-secondary structures.

(2-3) RPA3 Solvated in Deuterated Solutions in the Presence of DPPC. From 10 min to 4 h DPPC favors the NH exchange as 0.5 M NaCl (Figure 7). As discussed in part A-3-3, in 10 min internal CO groups are no longer NH bonded. The corresponding NH groups are supposed to be in interaction with the polar or with the ionic sites of DPPC. They are assumed to be rapidly exchangeable and then would correspond to the ≅8% additional exchanged NH groups measured when RPA3 is solvated in DPPC–^2H_2O instead of pure ^2H_2O. From 10 min to 4 h the distance between the two curves remains unchanged, whereas from 4 h to 24 h the DPPC–^2H_2O curve tends to approximate the ^2H_2O curve. This suggests that parts of RPA3 that interact with DPPC are solvated earlier in DPPC–^2H_2O than in pure ^2H_2O. We thus assume that these exchangeable domains, which were previously located in polar internal parts of RPA3, become more accessible to ^2H_2O when the protein is associated with lipids. As in pure ^2H_2O, the 29% nonexchanged NH groups at 24 h are attributed to hydrogen-bonded NH groups located in apolar regions of the protein. These assumptions are in agreement with the results reported in part A-3-3. They are not consistent with an enhancement of RPA3 β-structures induced by DPPC but are in favor of an enhancement of ^2H_2O solvation between 10 min and 4 h.

In a DPPC–NaCl–^2H_2O environment, the NH ↔ N^{2}H exchange is even more favored than in any of the preceding solvents. Compared to the results obtained in DPPC–^2H_2O the NaCl effect becomes sensitive only after 30 min and reaches a maximum at 4 h. Rather than a change in the repartition of β-structures, these results support the assumption proposed in part A-3-3 that, in the presence of DPPC, even low NaCl concentrations favor interactions between ^2H_2O and peptide units in polar parts of RPA3.

Concluding Remarks

Analysis of the structure and solvation of RPA3 has been established both from the absorption measurements in the amide I* frequency range and from quantitative estimations of NH ↔ N^{2}H peptidic exchange. In itself, neither of these two methods of analysis is supposed to give absolute results, but as all the experiments were held under the same conditions of protein concentration, pH, and temperature, and as both kinds of investigations have been carefully related to each other, the overall study is assumed to give a coherent description of the conformational dynamics of RPA3 lectin when the protein is dissolved in various detuerated media. Hence, even weak variations observed from one solution to another have been reliably analyzed.

Compared to most of the infrared studies reported on proteins, some relatively unusual assignments in the amide I region have been proposed. First, the higher amide I* components (1684–1671 cm^{-1}), the frequency of which depends on the solvent used, have been mostly associated with "free" CO groups, which are rapidly solvated by ^2H_2O. The occurrence of these "free" CO groups is correlated with that of "free" NH groups. The presence of these NH groups was confirmed by the NH ↔ N^{2}H exchange data. Second, from the occurrence of two components in the 1600–1640-cm^{-1} range and from the NH ↔ N^{2}H exchange two β-structures were discriminated: antiparallel β-sheets of large size and less stable parallel and/or antiparallel β-strands of smaller size. The large antiparallel β-structures give rise to absorption observed between 1600 and 1620 cm^{-1} (Chirgadze et al., 1973; Byler & Susi, 1986). The two other β-structures are indistinctively related to the component of ca. 1635 cm^{-1} (Susi & Byler, 1987). Naik and Krimm (1986) have associated similar frequencies to β-helical structures present in D,L polypeptides. However, such structures could not be retained for RPA3. Third, all the assignments proposed to analyze the solvation process of RPA3

emphasize the importance of peptide unit–solvent interactions. The lifetime of these interactions may be shorter than the lifetime of the interactions involved in the cooperative stabilization of secondary structures, but is long enough to induce internal and external conformational fluctuations of the protein (Frauenfelder & Gratton, 1986; Pace, 1986; Segawa & Kume, 1986). Recently peptide unit–^2H_2O interactions have been hypothesized to explain the amide I frequency of proteins (Jakobsen et al., 1986; Poole & Barlow, 1986; Castresana et al., 1987; Casal et al., 1988; Trewhella et al., 1989). The effects of direct peptide unit–ion interactions on protein conformations are less currently discussed (Schellman, 1987) although salt effects on the NH $\leftrightarrow$ N^2H peptidic exchange have been demonstrated (Kim & Baldwin, 1982; Kim, 1986).

In an anhydrous state RPA3 displays a high content of β-secondary structure. β-Structures of small size located in polar domains account for $\cong$35% of RPA3 skeleton, and short β-strands and larger β-sheets localized in apolar domains for 25%.

Analyses of the conformations adopted in different aqueous media indicate that RPA3 is a flexible molecule. When RPA3 is dissolved in ^2H_2O some of the "free" peptide units observed in the lyophilized form as well as peptide groups involved in weak peripheral hydrogen bonds located in turns or β-structures of small size are rapidly solvated. β-Structures of small size located in polar internal regions of RPA3 are lately disrupted and hydrated. Both low and high NaCl concentrations prevent RPA3 precipitation. However, only NaCl concentrations of $\leq$0.15 M limit the progressive local unfolding of RPA3 and protect the inner secondary structure from direct ^2H_2O contact, probably through a process known as the "salting in" effect (Von Hippel & Schleich, 1969) by which the salt may limit local electrostatic repulsion forces by neutralizing amino acid side-chain charges. In contrast, NaCl concentrations of >0.15 M lead to direct peptide unit–ion interactions. This phenomenon appears different from the classical "salting out" effect, where proteins tend to precipitate in their native or active forms as the salt concentrations increase.

Moreover RPA3 lectin was shown to interact with DPPC molecules through direct polar interactions between peptide units and the polar heads (PO_4H^-/PO_4^{2-}) of DPPC. These peptide units are assumed to be located in polar regions of RPA3. The presence of NaCl under these conditions modifies both the structure of the lipid multilayers and the lectin conformation (Surewicz et al., 1987). This could be related to data reported by Freier and Rüdiger (1987) and Kummer and Rüdiger (1988). These authors showed that two lectin-binding storage protein fractions can be distinguished in lentil (Freier & Rüdiger, 1987) and pea (Kummer & Rüdiger, 1988) seeds, a nonglycosylated one, which binds to the lectin by ionic forces, and a glycosylated one, which interacts by the carbohydrate binding site. It has recently appeared that lectins are bifunctional molecules that may interact with well-defined carbohydrate structures by the "classical" specific binding but may also interact with other proteins by polar and/or possibly hydrophobic interactions. Both the lectin–carbohydrate and the lectin–protein interactions have been shown to be biologically significant (Barondes, 1988). A vibrational study of the aliphatic side chains of DPPC would indicate if the apolar part of RPA3 may be embedded in lipid bilayers or not and would contribute to progress in the knowledge of lectin structure–function relationship.

Acknowledgments

We thank B. Beccart (Nicolet Society) who performed the self-deconvolution and second-derivative analyses.

Registry No. DPPC, 2644-64-6.

References

Bandekar, J., & Krimm, S. (1988a) *Biopolymers 27*, 909–921.
Bandekar, J., & Krimm, S. (1988b) *Biopolymers 27*, 885–908.
Baron, M.-H., de Lozé, C., & Sagon, G. (1973) *J. Chim. Phys. 70*, 1509–1517.
Baron, M.-H., de Lozé, C., Toniolo, C., & Fasman, G. D. (1978) *Biopolymers 17*, 2225–2239.
Barondes, S. H. (1988) *Trends Biochem. Sci. 13*, 480–482.
Biay, I., Attane, J.-C., & Vitoux, B. (1989) *Proceedings of the Third European Conference on the Spectroscopy of Biological Molecules*, Bologna, Italy (Bertoluzza, A., Fagnano, C., & Monti, P., Eds.) pp 85–86, Esculapio, Bologna.
Blume, A., Hübner, W., & Messner, G. (1988) *Biochemistry 27*, 8239–8249.
Byler, D. M., & Susi, H. (1986) *Biopolymers 25*, 469–487.
Byler, D. M., & Susi, H. (1988) *J. Ind. Microbiol. 3*, 73–88.
Casal, H. L., Köhler, U., & Mantsch, H. H. (1988) *Biochim. Biophys. Acta 957*, 11–20.
Castresana, J., Muga, A., Goni, F. M., & Arrondo, J. L. R. (1987) *Proceedings of the Second European Conference on the Spectroscopy of Biological Molecules*, Freiburg, West Germany (Schmid, E. D., Schneider, F. W., & Siebert, F., Eds.) pp 125–128, J. Wiley, New York.
Chirgardze, Y. N., & Nevskaya, N. A. (1976) *Biopolymers 15*, 627–636.
Chirgardze, Y. N., Shestopalov, B. V., & Venyaminov, S. Y. (1973) *Biopolymers 12*, 1337–1351.
Chirgardze, Y. N., Fedorov, O. V., & Trushina, N. P. (1975) *Biopolymers 14*, 679–694.
De Lozé, C., Baron, M.-H., & Fillaux, F. (1978) *J. Chim. Phys. 75*, 631–649.
Eckert, K., Grosse, R., Malur, J., & Repke, K. R. H. (1977) *Biopolymers 16*, 2549–2563.
Einhoff, W., Fleischmann, G., Freier, T., Kummer, H., & Rüdiger, H. (1986) *Biol. Chem. Hoppe-Seyler 367*, 15–25.
Fillaux, F., & de Lozé, C. (1972) *Biopolymers 11*, 2063–2077.
Fleischmann, G., & Rüdiger, H. (1986) *Biol. Chem. Hoppe-Seyler 367*, 27–32.
Frauenfelder, H., & Gratton, E. (1986) *Methods Enzymol. 127*, 207–216.
Freier, T., & Rüdiger, H. (1987) *Biol. Chem. Hoppe-Seyler 368*, 1215–1223.
Goldstein, I. J., & Poretz, R. D. (1986) in *The Lectins: Properties, Functions and Applications in Biology and Medicine* (Liener, I. E., Sharon, N., & Goldstein, I. J., Eds.) pp 33–247, Academic Press, New York.
Gregory, R. B., & Rosenberg, A. (1986) *Methods Enzymol. 131*, 448–508.
Herrmann, M. S., Richardson, C. E., Setzler, L. M., & Behnke, W. D. (1978) *Biopolymers 17*, 2107–2120.
Herskovits, T. T., & Mescanti, L. (1965) *J. Biol. Chem. 240*, 639–644.
Hume, D. A., & Weidemann, M. J. (1980) in *Research Monographs in Immunology 2*, Elsevier North/Holland Biomedical Press, Amsterdam.
Jackson, M., Haris, P. I., & Chapman, D. (1989) *J. Mol. Struct. 214*, 329–355.
Jakobsen, R. J., Wasacz, F. M., & Brasch, J. W. (1986) *Biopolymers 25*, 639–654.
Kauppinen, J. K., Moffatt, D. J., Mantsch, H. H., & Cameron, D. G. (1981) *Appl. Spectrosc. 35*, 271–275.

Kim, P. S. (1986) *Methods Enzymol. 131*, 136-156.
Kim, P. S., & Baldwin, R. L. (1982) *Biochemistry 21*, 1-5.
Krimm, S., & Bandekar, J. (1986) *Adv. Protein Chem. 38*, 181-364.
Kummer, H., & Rüdiger, H. (1988) *Biol. Chem. Hoppe-Seyler 369*, 639-646.
Lis, H., & Sharon, N. (1984) in *Biology of Carbohydrates* (Ginsburg, V., & Robbins, P., Eds.) Vol. 2, pp 1-86, J. Wiley, New York.
Lotta, T. I., Salonen, I. S., Virtanen, J. A., Eklund, K. K., & Kinnunen, P. K. J. (1988) *Biochemistry 27*, 8158-8169.
Naik, V. M., & Krimm, S. (1986) *Biophys. J. 49*, 1131-1145.
Pace, C. N. (1986) *Adv. Enzymol. 131*, 266-280.
Perchard, C., Baron, M.-H., & de Lozē, C. (1984) *J. Mol. Struct. 112*, 247-262.
Pêre, M., Bourrillon, R., & Jirgensons, B. (1975) *Biochim. Biophys. Acta 393*, 31-36.
Poole, P. L., & Barlow, D. J. (1986) *Biopolymers 25*, 317-335.
Schellman, J. A. (1987) *Biopolymers 26*, 549-559.
Segawa, S. I., & Kume, K. (1986) *Biopolymers 25*, 1981-1996.
Sharif, A., Brochier, J., & Bourrillon, R. (1977) *Cell. Immunol. 31*, 302-310.
Strosberg, A. D., Buffard, D., Lauwereys, M., & Foriers, A. (1986) in *The Lectins: Properties, Functions and Applications in Biology and Medicine* (Liener, I. E., Sharon, N., & Goldstein, I. J., Eds.) pp 249-264, Academic Press, New York.
Surewicz, W. K., & Mantsch (1988) *Biochim. Biophys. Acta 952*, 115-130.
Surewicz, W. K., Moscarello, M. A., & Mantsch, H. H. (1987) *Biochemistry 26*, 3881-3886.
Susi, H., & Byler, D. M. (1987) *Arch. Biochem. Biophys. 258*, 465-469.
Trewhella, J., Liddle, W. K., Heidorn, D. B., & Strynadka, N. (1989) *Biochemistry 28*, 1294-1301.
Von Hippel, P. H., & Schleich, T. (1969) in *Structure and Stability of Biological Macromolecules* (Timasheff, S. N., & Fasman, G. D., Eds.) pp 417-574, M. Dekker, New York.
Wantyghem, J., Goulut, C., Frênoy, J.-P., Turpin, E., & Goussault, Y. (1986) *Biochem. J. 237*, 483-489.

Structure of Yeast Triosephosphate Isomerase at 1.9-Å Resolution[†,‡]

Elias Lolis, Tom Alber,[§] Robert C. Davenport,[∥] David Rose,[⊥] Fred C. Hartman,[#] and Gregory A. Petsko*
Department of Chemistry, Massachusetts Institute of Technology, Cambridge, Massachusetts 02139
Received June 30, 1989; Revised Manuscript Received December 11, 1989

ABSTRACT: The structure of yeast triosephosphate isomerase (TIM) has been solved at 3.0-Å resolution and refined at 1.9-Å resolution to an *R* factor of 21.0%. The final model consists of all non-hydrogen atoms in the polypeptide chain and 119 water molecules, a number of which are found in the interior of the protein. The structure of the active site clearly indicates that the carboxylate of the catalytic base, Glu 165, is involved in a hydrogen-bonding interaction with the hydroxyl of Ser 96. In addition, the interactions of the other active site residues, Lys 12 and His 95, are also discussed. For the first time in any TIM structure, the "flexible loop" has well-defined density; the conformation of the loop in this structure is stabilized by a crystal contact. Analysis of the subunit interface of this dimeric enzyme hints at the source of the specificity of one subunit for another and allows us to estimate an association constant of 10^{14}-10^{16} M^{-1} for the two monomers. The analysis also suggests that the interface may be a particularly good target for drug design. The conserved positions (20%) among sequences from 13 sources ranging on the evolutionary scale from *Escherichia coli* to humans reveal the intense pressure to maintain the active site structure.

Yeast triosephosphate isomerase (TIM;[1] EC 5.3.1.1) is a dimer of identical subunits, each of molecular weight about 26 000. There is no evidence for catalytic cooperativity between the two subunits. It has been shown, however, that the enzyme is only active as a dimer (Waley, 1973; Casal et al., 1987). TIM is the glycolytic enzyme that catalyzes the isomerization of the two products of aldolase, D-glyceraldehyde 3-phosphate and dihydroxyacetone phosphate. Since only GAP continues to proceed along the glycolytic pathway, TIM is absolutely essential for efficient energy production. There are no reported cases of organisms devoid of triosephosphate isomerase activity. Indeed, people who are defective in one of the alleles for the TPI gene are found to suffer from chronic hemolytic anemia and neuromuscular disorders (Valentine et al., 1983).

Triosephosphate isomerase has been the subject of extensive biophysical studies. The free energy profile of the chicken

[†] The research of G.A.P. was supported by grants from NIH and that of F.C.H. by the Office of Health and Environmental Research, U.S. Department of Energy, under Contract DE-AC05-84OR21400 with the Martin Marietta Energy Systems, Inc. We also acknowledge Berlex Laboratories for providing a fellowship for one of us (E.L.).
[‡] Crystallographic coordinates have been submitted to the Brookhaven Protein Data Bank.
[§] Present address: Department of Biochemistry, University of Utah School of Medicine, Salt Lake City, UT 84132.
[∥] Present address: Department of Biology, Massachusetts Institute of Technology, Cambridge, MA 02139.
[⊥] Present address: Division of Biological Sciences, National Research Council, Ottawa, Canada K1A 0R6.
[#] Permanent address: Biology Division, Oak Ridge National Laboratory, Oak Ridge, TN 37830.

[1] Abbreviations: DHAP, dihydroxyacetone phosphate; GAP, D-glyceraldehyde 3-phosphate; rms, root mean square; TIM, triosephosphate isomerase; TPI, gene coding for triosephosphate isomerase.

0006-2960/90/0429-6609$02.50/0